

# Enhancing Light Emission of ZnO Microwire-Based Diodes by Piezo-Phototronic Effect

Qing Yang,<sup>†,‡</sup> Wenhui Wang,<sup>†</sup> Sheng Xu,<sup>†</sup> and Zhong Lin Wang<sup>\*,†</sup>

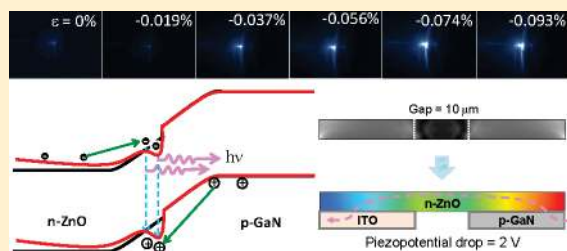
<sup>†</sup>School of Material Science and Engineering, Georgia Institute of Technology, Atlanta, Georgia 30332-0245, United States

<sup>‡</sup>State Key Laboratory of Modern Optical Instrumentation, Department of Optical Engineering, Zhejiang University, Hangzhou 310027, China

**S** Supporting Information

**ABSTRACT:** Light emission from semiconductors depends not only on the efficiency of carrier injection and recombination but also extraction efficiency. For ultraviolet emission from high band gap materials such as ZnO, nanowires have higher extraction efficiencies than thin films, but conventional approaches for creating a p–n diode result in low efficiency. We exploited the noncentral symmetric nature of n-type ZnO nanowire/p-type GaN substrate to create a piezoelectric potential within the nanowire by applying stress. Because of the polarization of ions in a crystal that has noncentral symmetry, a piezoelectric potential (piezopotential) is created in the crystal under stress. The piezopotential acts as a “gate” voltage to tune the charge transport and enhance carrier injection, which is called the piezo-phototronic effect. We propose that band modification traps free carriers at the interface region in a channel created by the local piezoelectric charges. The emission intensity and injection current at a fixed applied voltage have been enhanced by a factor of 17 and 4, respectively, after applying a 0.093% compressive strain and improved conversion efficiency by a factor of 4.25. This huge enhanced performance is suggested arising from an effective increase in the local “biased voltage” as a result of the band modification caused by piezopotential and the trapping of holes at the interface region in a channel created by the local piezoelectric charges near the interface. Our study can be extended from ultraviolet range to visible range for a variety of optoelectronic devices that are important for today’s safe, green, and renewable energy technology.

**KEYWORDS:** LED, nanowire, GaN, ZnO, piezo-phototronic effect, piezoelectric effect



High-efficient ultraviolet (UV) emitters are required for applications in chemical, biology, aerospace, military, and medical technologies. Although, the internal quantum efficiency of UV LED is as high as 80%, the external efficiency for a conventional single p–n junction thin-film based LED is only about 3% due to the low extraction efficiency (about  $1/4n^2$ , where  $n$  is the refraction index) as a result of total internal reflection.<sup>1,2</sup> The usage of ZnO nanowires (NWs) as active layers to fabricate nanosized heterojunction LED is expected to be an effective approach for improving extraction efficiency,<sup>3–8</sup> but the reported data so far show low external efficiency ( $\sim 2\%$ ), possibly due to the very low internal efficiency of NW based LED.

ZnO nanowires (NWs) have attracted a lot of interests owing to their unique semiconductor, photonic and piezoelectric properties for a range of applications in electronics, optoelectronics and energy harvesting.<sup>8–12</sup> The direct wide band gap ( $\sim 3.30$  eV) and large excitonic binding energy ( $\sim 60$  meV) as well as relative large refraction index make ZnO NWs a good candidate for high efficient light emitting diodes,<sup>3–8</sup> photodetectors<sup>13,14</sup> and solar cells.<sup>15,16</sup> Because of the polarization of ions in ZnO that has noncentral symmetry, a piezoelectric potential (piezopotential) is created in the crystal by applying a stress. Recently, by utilizing the coupling of

piezoelectric and semiconducting properties of ZnO, piezotronic devices based on ZnO NWs, such as nanogenerators,<sup>17,18</sup> piezoelectric field effect transistors,<sup>19,20</sup> and piezoelectric diodes<sup>21,22</sup> have been developed, which rely on the tuning/controlling effect of piezopotential on the charge transport properties across an interface for fabricating new functional devices. Furthermore, piezopotential has been utilized to enhance the performance of optoelectronic devices, such as the output of a photocell<sup>23,24</sup> and sensitivity of a photodetector,<sup>25,26</sup> resulting in a new field named piezo-phototronics.<sup>10</sup> Piezo-phototronic effect is to use the inner-crystal piezopotential as a “gate” voltage to tune/control the charge transport and photonic behaviors for optimizing the device performance with considering the presence of strain in flexible/stretchable electronic devices fabricated on soft substrates.

Here we demonstrate how the piezo-phototronic effect can be effectively utilized to enhance the external efficiency of an LED fabricated using a single ZnO micro/nanowire on a GaN substrate. The emission light intensity and injection current at a fixed applied voltage has been enhanced by a factor of 17 and 4 after applying a

**Received:** July 30, 2011

**Published:** August 08, 2011

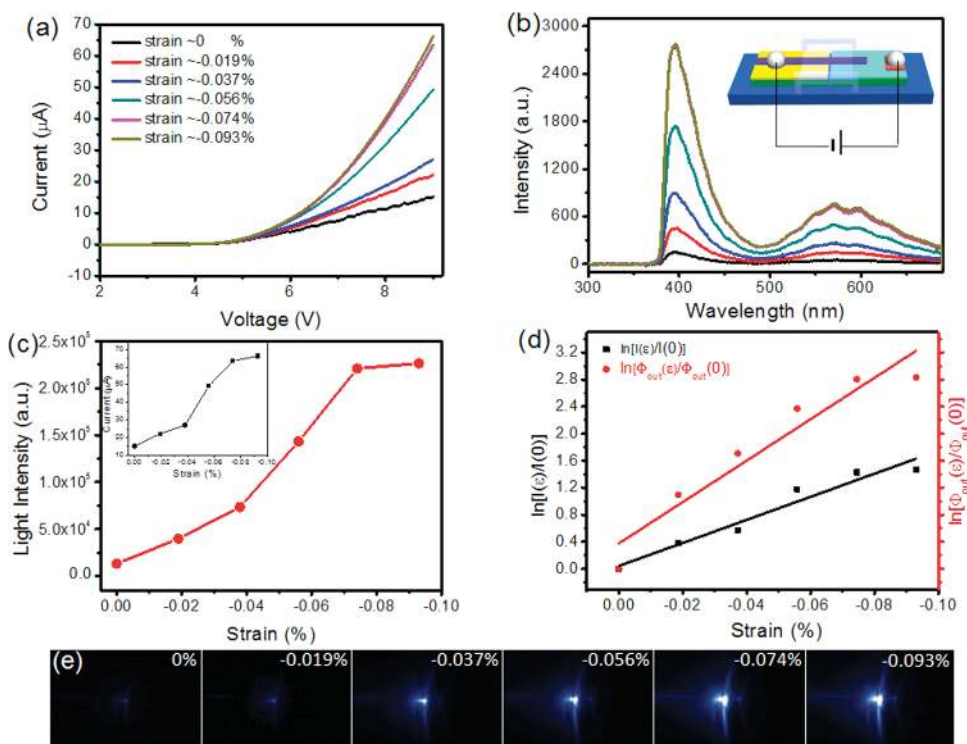


**Figure 1.** Enhancement of emission light intensity and conversion efficiency of a (n-ZnO wire)–(p-GaN film) LED under applied strain. A schematic diagram of the fabricated device is inset in (b). (a)  $I$ – $V$  characteristics of the device at forward bias with the variation of the applied strain; and (b) the corresponding optical spectra of the emitted light at a bias of 9 V. (c) Integrated emission light intensities from the data shown in (b), showing a huge increase in the emission intensity with the increase of the applied compressive strain. The inset is the injection current of the LED at 9 V biasing voltage with the increase of the strain. (d) Change in relative injection current  $\ln[I(\varepsilon)/I(0)]$  and relative emission light intensity  $\ln[\Phi_{\text{out}}(\varepsilon)/\Phi_{\text{out}}(0)]$  under different strain. The LED efficiency has been increased by a factor of 4.25 at the maximum applied strain in comparison to the zero strain case. (e) CCD images recorded from the emitting end of a packaged single wire LED under different applied strain.

0.093% compressive strain, respectively, and the corresponding conversion efficiency was improved by a factor of 4.25. This is suggested arising from an effective increase in the local “biased voltage” as a result of the band modification caused by piezopotential and the trapping of free carriers at the interface region in a channel created by the piezopotential near the interface. Furthermore, the piezoresistance and piezooptic (photoelastic) effects have been utilized to simultaneously tune the light emitting intensity, spectra, and polarization. Our study shows that the piezo-phototronic effect can be effectively used for enhancing the efficiency of energy conversion in today’s safe, green, and renewable energy technologies.

Our experiments were carried out based on the following design. A single ZnO micro/nanowire LED was fabricated by manipulating a wire on a trenched substrate (see Section A in Supporting Information). A Mg doped p-type GaN film epitaxially grown on a sapphire substrate by metalorganic chemical vapor deposition (MOCVD) was used to form a p–n junction with n-type ZnO wire. An ITO coated sapphire substrate was used as the cathode that was placed side-by-side with the GaN substrate with a well-controlled gap (see the inset in Figure 1b). The ZnO wire was placed across the gap with a close contact with GaN. A transparent polystyrene (PS) tape was used to cover the nanowire. A normal force was applied on the PS film by an alumina rod connected to a piezo nanopositioning stage. In this case, a compressive stress was applied uniformly normal to the interface between the side surface of the ZnO wire and the GaN substrate surface; such a compressive force along the  $a$ -axis of the ZnO wire resulted in a tensile strain along the  $c$ -axis, the growth direction of

the wire. In this design, there was no transverse bending or twist on the wire to ensure the stability of the p–n junction interface between the ZnO wire and GaN substrate.

The  $I$ – $V$  characteristics, dependence of emission intensity on the applied voltage and the features of the characteristic peaks of an as-fabricated LED without applying additional strain are presented in the Supporting Information. The external efficiency of an as-fabricated single wire LED was measured conservatively to be  $\sim 1.84\%$  before applying a strain (Table 1), which is as high as that for a single p–n junction based UV LED.<sup>1–8</sup> To test the strain effect on a single ZnO wire LED, we systematically investigated its output light intensity, electroluminescence spectra and polarization as the strain being applied. At a fixed applied bias above the turn-on voltage (3 V), the current and light emission intensity increased obviously with increase of the compressive strain (Figure 1a,b). The significantly enhanced light intensity can also be directly observed in optical images recorded by a CCD (Figure 1e). The  $\ln[I(\varepsilon)/I(0)]$  and  $\ln[\Phi_{\text{out}}(\varepsilon)/\Phi_{\text{out}}(0)]$  dependence on strain  $\varepsilon$  is shown in Figure 1d, where  $\Phi_{\text{out}}(\varepsilon)$  and  $I(\varepsilon)$  are the light intensity and injection current of the LED under strain, respectively; and  $\Phi_{\text{out}}(0)$  and  $I(0)$  are the corresponding quantities of the as-fabricated LED without applying an external strain; both curves have a linear relationship with external strain, and the slope of  $\ln[\Phi_{\text{out}}(\varepsilon)/\Phi_{\text{out}}(0)] - \varepsilon$  is larger than that of  $\ln[I(\varepsilon)/I(0)] - \varepsilon$ , indicating a clear increase in light conversion efficiency. The injection current and output light intensity were largely enhanced by a factor of 4 and 17, respectively, after applying a 0.093%  $a$ -axis compressive strain, indicating that the conversion

efficiency was improved by a factor of 4.25 in reference to that without applying strain. This means that the external true efficiency of the LED can reach  $\sim 7.82\%$  after applying a strain, which is comparable to that of the LED structures based on nanorods enhanced hybrid quantum wells LED.<sup>27</sup>

To confirm the validity of the observed data, the stability of the contact between ZnO wire and GaN was carefully examined by repeating the applied strain (see Section C in Supporting Information). Once the strain was retracted, the light emission intensity dropped back to the value observed at strain free case (Supporting Information Figure S7b). A linear relationship observed in the enhancement factor with strain (Figure 1d) proved that a possible change in contact area between n- and p-side of the device was not responsible to the observed increase in efficiency.

The enhancements of the distinct emission bands are analyzed as a function of the applied strain using the peak-deconvolution method (Figure 2a). The analysis of the emission origin is presented in the section D of Supporting Information. The emission coming from the ZnO-GaN interface grew fastest among four emission bands, due to the trapping of free carriers in the channel near the interface. The ratio of the UV-to-visible emission increased exponentially with the increase of the in-plane

compressive strain (Figure 2d), since the UV/blue near band edge emission is more sensitive to the band structure change than the defect centers. The peak positions of the four emission bands did not exhibit any appreciable shift under straining (Figure 2c), but they did have obvious blue shift as the applied bias voltage was increased (Figure S5c in Supporting Information). These results indicated that the effect of strain on the LED is different with the effect of increase applied bias voltage on it.

When the n-ZnO wire/p-GaN substrate LED is under axial straining, two typical effects influence the output light intensity and spectra. One is the piezoresistance effect, which is caused by the change in bandgap and possibly density of states in the conduction band. This effect acts as adding a serial resistance to the LED. The second effect is the piezo-phototronic effect,<sup>10</sup> which is about the tuning of the optoelectronic process at the interface using the piezopotential created along the ZnO wire. ZnO has a noncentral symmetric crystal structure, in which the cations and anions are tetrahedrally coordinated. A straining on the basic unit results in a polarization of the cations and anions, which is the cause of the piezopotential inside the crystal. As for the ZnO (n-type)-GaN (p-type) LED, a schematic diagram of its band structure is presented in Figure 3a. Since the size of the GaN substrate is much larger than that of the ZnO microwire, the strain in GaN is much smaller than that in ZnO, thus our discussions mainly focus on the piezoelectric effect from ZnO. Under an assumption of no-doping or low-doping in ZnO for simplicity, numerically calculated piezopotential distribution in the ZnO microwire shows (Figure 3b, see section E in Supporting Information for the fundamental theory of the calculation) that a negative potential drop is created along its length when the ZnO microwire is under *a*-axis compressive strain. The finite doping in the wire may partially screen the piezoelectric charges, but it cannot totally eliminate the piezoelectric potential if the doping level is low, thus

**Table 1. Calculated External Efficiency of a Single Wire LED without Strain**

applied voltage (V)	injection current ( $\mu\text{A}$ )	measured emission power ( $\mu\text{W}$ )	external efficiency (%)
7	0.59	0.08	1.94
8	1.47	0.23	1.96
10	7.26	1.42	1.96
11	11.48	1.91	1.51

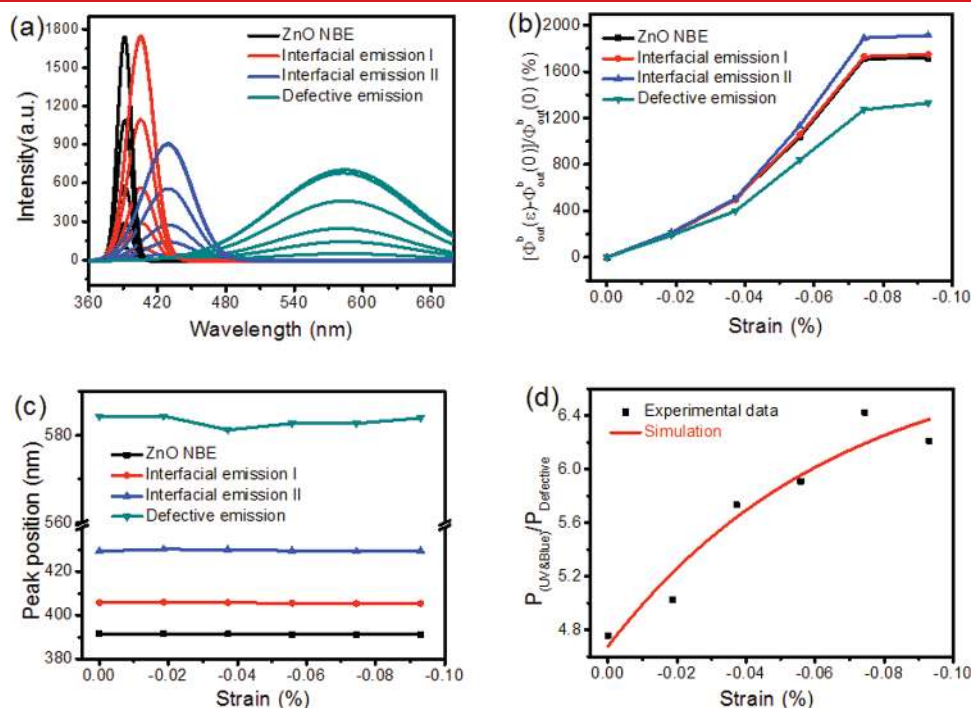


**Figure 2.** Quantifying the spectra of the emitted light from a (n-ZnO wire)-(p-GaN film) LED under different applied strain. (a) The four emission bands derived using deconvolution from the data shown in Figure 1b. (b) Change in relative peak height as a function of the external strain. (c) Dependence of the peak position on the applied strain. (d) The ratio of the emitted UV-to-visible intensities as a function of the strain.



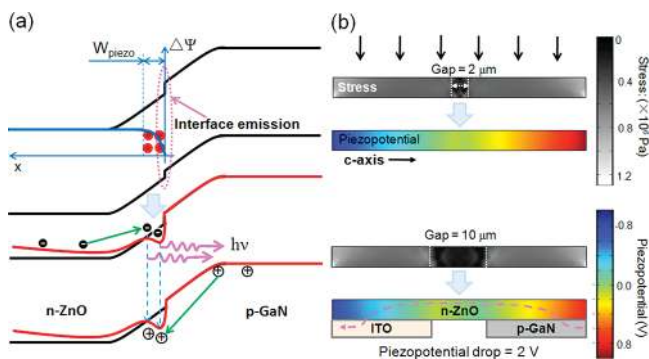


**Figure 3.** Proposed mechanism of the enhanced light emission under strain for a (n-ZnO wire)–(p-GaN film) LED. (a) Schematic energy band diagram of the p–n junction without (upper) and with (lower, red line) applied compressive strain, where the channel created at the interface inside ZnO is due to the piezopotential created by strain (see section E in Supporting Information). The blue line presents the potential profile along the  $x$ -axis (the  $c$ -axis of ZnO wire) assuming positive piezo-charges distribute within a width of  $W_{\text{piezo}}$  adjacent to the interface. The red dots represent the local piezo-charges near the interface, which produces a carrier trapping channel. The slope of the red line in the lower image at the ZnO side represents the driving effect of piezopotential to the movement of the charge carriers. (b) Simulated stress and piezopotential distributions in the ZnO wire with a gap distance of 2 and 10  $\mu\text{m}$  (see the schematic inset in Figure 1b), respectively, under an externally applied compressive stress of 1 MPa. The finite-element analysis method (COMSOL) is used to calculate the stress and piezopotential in the wire. The diameter and length used for calculation are 4 and 50  $\mu\text{m}$ , respectively. The conductivity of the ZnO is ignored in the simulation for simplicity.

a dip in the band is possible. This is proved by the numerous studies we have carried out for nanogenerators and piezotronics. The low-doping in ZnO wire here is consistent with our experiment results because the ZnO wire is fabricated by a high-temperature thermal evaporation process using pure ZnO powders as the source.<sup>28</sup> If the  $c$ -axis of the ZnO wire is pointing from the ITO side to the GaN side, as labeled in Figure 3b, the effect of the local negative piezopotential at the ITO side is equivalent to applying an extra forward biased voltage on the device. Thus, the depletion width and internal field are reduced under this additional component of forward biased voltage. Subsequently, the injection current and emitting light intensity under the same externally applied forward voltage increase when the device is strained. Alternatively, if the  $c$ -axis of the ZnO wire is reversed and pointing away from the GaN side, the GaN side has a lower piezopotential, which is equivalent to applying an extra reversely biased voltage on the device. The depletion width and internal field are thus increased, resulting in a reduction of the injection current and emitting light intensity with the increase of the applied strain. Experimentally, when manipulating the wires for fabricating devices, about 50% of them have the  $c$ -axis of the wires pointing from the ITO side to the GaN side, while the other 50% pointing in the reverse direction. For the 20 devices we have measured, about 50% of the devices showed enhanced light emitting when strained, while the remaining had reduced light-emitting intensity (see Section C2 in Supporting Information), consistent with the expected results. This fact also indicates that the observed enhancement in light emission is dominated by polar piezopotential effect rather than any nonpolar effects such as change in contact-area and/or piezoresistance.

It is known that the light output of LED is proportional to the external efficiency and injection current.<sup>29</sup> Meanwhile, the injection current across the p–n junction increases exponentially with the increase of the forward bias voltage (for  $V \gg kT/q$ ) according to the Shockley equation.<sup>30</sup> Therefore, the change in light emission intensity under strain can be described by (see Section E in Supporting Information for details):

$$\begin{aligned} \ln\left(\frac{\Phi_{\text{out}}(\varepsilon)}{\Phi_{\text{out}}(0)}\right) &= \ln\left(\frac{I(\varepsilon)}{I(0)}\right) + \ln\left(\frac{\eta_{\text{ex}}(\varepsilon)}{\eta_{\text{ex}}(0)}\right) \\ &= \frac{\Delta\psi}{kT} + f(\varepsilon) \end{aligned} \quad (1)$$

where  $\eta_{\text{ex}}(\varepsilon)$  and  $\eta_{\text{ex}}(0)$  represent the output external efficiency of LED with and without applying a strain, respectively,  $k$  is the Boltzmann constant,  $T$  is temperature, and  $f(\varepsilon)$  represents the effect of strain on external efficiency. It is expected that the  $\ln[\Phi_{\text{out}}(\varepsilon)/\Phi_{\text{out}}(0)] - \varepsilon$  and  $\ln[I(\varepsilon)/I(0)] - \varepsilon$  have a linear relationship with the external strain, as shown by experimental data in Figure 1d.

The enhancement factor for light emission was larger than that for the injection current (Figure 1d), which means that the quantum efficiency was enhanced with the increase of strain (eq 1). By solving Poisson equation with coupling piezoelectric effect (see Section E in Supporting Information for details), the enhancement of external efficiency may be caused by the localized positive piezopotential near GaN/ZnO interface, which produces carrier trapping channels (see Figure 3a). Electrons and holes can be temporarily trapped and accumulated in the channels in the conduction and valence band, respectively. Since abundant electrons are available in ZnO, for instance, the efficiency of the LED is largely dominated by the local concentration of holes because of the high activation energy of the most commonly used acceptor dopants (Mg) in GaN ( $\sim 200$  meV).<sup>31</sup> The trapped holes may increase the hole injection from p-GaN into n-ZnO, which increases the recombination efficiency of electrons and holes near the junction, resulting in a large increase in emission intensity. It is pointed out that although the absolute values of the band offset varies in different reports<sup>4,6,32–34</sup> and is dependent on the fabrication process of the heterojunction, the band offset values do not affect the tendency of the band modification and the profile of the carrier trapping channel by piezopotential.

The peak positions of the four emission bands did not exhibit any appreciable shift under straining (Figure 2c), but they did have obvious blue shift as the applied bias voltage was increased (see Section B in Supporting Information). It is known that the bandgap of ZnO decreases under compressive  $a$ -axis strain,<sup>35–37</sup> while the bandgap of GaN also decreases under compressive  $c$ -axis strain.<sup>38,39</sup> In this case, the peak position should have a red shift under compressive strain. On the other hand, the emission centers of the n-ZnO/p-GaN LED have blue shift with the increase of injection current due to the band renormalization, band filling at high current and/or the increased kinetic energies of electrons and holes.<sup>6</sup> When these two complementary effects coexist, one may balance the other, resulting in negligible shift in emission peaks.

The change in refractive index of ZnO is also possible under strain, which is the photoelastic effect. We investigated the photoelastic effect by studying the polarization behavior of the emission under applied strain. Figure 4a shows the electroluminescence intensity of a single wire LED as a function of the rotation angle of the polarizer in reference to the orientation of the wire. If  $\Phi_{\text{out}}^{\parallel}$  and  $\Phi_{\text{out}}^{\perp}$  represent the intensities of the

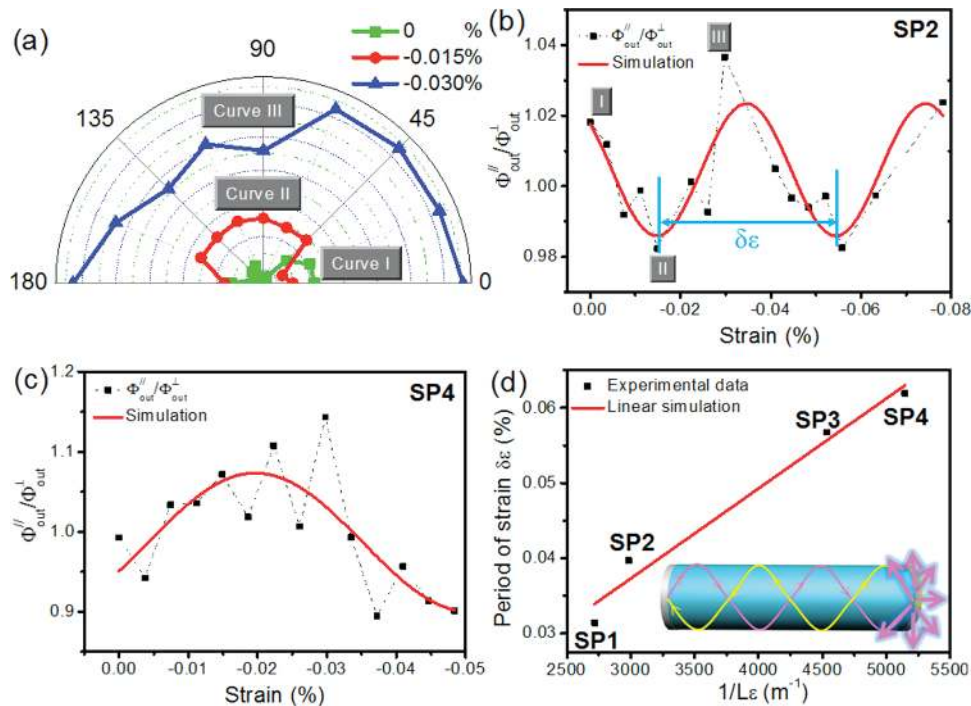


**Figure 4.** Effects of strain on the polarization of the (n-ZnO wire)–(p-GaN film) emitted light. (a) Beam profile for the LED output under different strain as a function of the polarization angle. (b) The  $\Phi_{\text{out}}^{\parallel}/\Phi_{\text{out}}^{\perp}$  ratio of the device used for (a) under different strain, where the points corresponding to the curves I–III are labeled I–III marked. The period at which the intensity ratio varies is defined as  $\delta\epsilon$ . (c) The  $\Phi_{\text{out}}^{\parallel}/\Phi_{\text{out}}^{\perp}$  ratio of device SP4 under different strain. (d) Plot of the measured strain varying period  $\delta\epsilon$  vs the inverse of the effective length of the ZnO wire under strain. The inset shows a schematic standing wave within a Fabry–Perot cavity (ZnO wire) for the  $P_{\perp}$  modes.

emission light when the polarization direction parallel ( $P_{\parallel}$  modes) and perpendicular ( $P_{\perp}$  modes) to the wire, respectively, the dependence of  $\Phi_{\text{out}}^{\parallel}/\Phi_{\text{out}}^{\perp}$  on strain can be fit using a function of sine square (Figure 4b,c and Supporting Information Figure S11), which may correspond to the resonance phenomenon of the Fabry–Perot cavity inside the wire, as described in follows.

Spontaneous emission from LED is polarized at various angles, but the guiding modes propagating along the ZnO wire are dominated by the  $P_{\perp}$  modes.<sup>40</sup> The propagating light along the wire may oscillate in the wire and interfere with each other due to end-surface reflection (Figure 4d inset). The change of refractive index under strain affects the optical path length of the propagating light, resulting in a modulation in the interference pattern inside the wire and in light emission. On the other hand, since the large aspect ratio of the wire (typically more than 100), the effect of strain on the optical path of the  $P_{\parallel}$  modes is much smaller than that on  $P_{\perp}$  modes. The ratio of  $\Phi_{\text{out}}^{\parallel}/\Phi_{\text{out}}^{\perp}$  can be described by the Airy equation<sup>41</sup> (see Section F in Supporting Information)

$$\Phi_{\text{out}}^{\parallel}/\Phi_{\text{out}}^{\perp}(\epsilon) \sim \left\{ 1 + \frac{4R}{(1-R)^2} \sin^2 \left[ \frac{\pi(2n_0L + n_0^3\beta E\epsilon L\epsilon)}{\lambda} \right] \right\} \quad (2)$$

where  $R$  is the reflectivity of ZnO wire at the end-face,  $n_0$  is its native refractive index without strain,  $L$  is the length of the wire,  $L_{\epsilon}$  is the effective length of the wire under strain (as shown in Supporting Information Figure S2),  $\beta$  is the photoelastic coefficients,  $E$  is Young's modulus of ZnO,  $\epsilon$  is the applied strain, and  $\lambda$  is the light wavelength. A simulation using eq 2 in reference to the data presented in Figures 4 and Supporting Information S11 derives the photoelastic coefficient  $\beta \sim 3.2 \times 10^{-12} \text{ m}^2/\text{N}$  (at a

wavelength of 395 nm) from the slope of the  $\delta\epsilon$  versus  $1/L_{\epsilon}$  curve (see eq S24 in Supporting Information), where  $\delta\epsilon$  is the strain period at which the  $\Phi_{\text{out}}^{\parallel}/\Phi_{\text{out}}^{\perp}$  oscillates (see Figure 4b). The  $\beta$  value is consistent to that reported for ZnO.<sup>42,43</sup> This study shows that it is possible to manipulate the polarization of a single wire LED through a proper externally applied strain.

Although our study has been focused on a single wire LED, an array of NWs with polarity control can be fabricated using a sweeping-printing-method<sup>44</sup> so that all of the NWs have the same  $c$ -axis orientation, and the nanowire array based LEDs can be fabricated on a polymer substrate for flexible LEDs,<sup>45</sup> through which a mechanical strain can be applied in a synchronized manner to uniformly enhance the output intensities of all NWs. Furthermore, electric driven polarized laser emission may also be possible by improving the reflectivity, increasing the driven current, improving the recombination efficiency, and solving the heating problem.

As a classical device, the performance of an LED is dictated by the structure of the p–n junction and the characteristics of the semiconductor materials. Once an LED is made, its efficiency is determined largely by the local charge carrier densities and the time at which the charges can remain at the vicinity of the junction. The latter is traditionally controlled by growing a quantum well or using a built-in electronic polarization for “trapping” electrons and holes in the conduction and valence bands,<sup>31,46</sup> respectively. Instead of using this prefabricated structure, we have introduced the piezopotential created in ZnO by strain to control the charge transport process at the ZnO–GaN interface, demonstrating the first LED whose performance is controlled by piezoelectric effect. The emission intensity and injection current at a fixed applied voltage have been enhanced by a factor of 17 and 4 after applying a 0.093% compressive strain, respectively, and the corresponding

conversion efficiency has been improved by a factor of 4.25 in reference to that without applying strain! Also, an external efficiency of 7.82% has been achieved. This hugely improved performance is not only attributed to the increase of injection current by the modification of the band profile, but also to the more elegant effect of the creation of a trapping channel for holes near the heterojunction interface, which greatly enhances the external efficiency. An increase in UV-to-visible ratio and stabilization of the peak position show that the spectrum quality is improved by external straining. In addition, the polarization of the output light has been modulated by the piezooptic effect. Our discovery is important not only for exploring the piezo-photonic effect through a three-way coupling among mechanical, electronical, and optical properties, but also can largely improve the efficiency and performance of LEDs and the design of a large range of optoelectronic devices based on ZnO and GaN with the use of their piezoelectric property.

## ■ ASSOCIATED CONTENT

**S Supporting Information.** Fabrication methods and measurement system, characterization of the as-fabricated LED before applying strain, evidence supporting the model presented, band diagram of the (n-ZnO wire)-(p-GaN film) heterojunction and analysis of the EL spectra, effect of strain on band profile of (n-ZnO wire)-(p-GaN film) heterojunction, and effect of strain on light propagation in ZnO wire. This material is available free of charge via the Internet at <http://pubs.acs.org>.

## ■ AUTHOR INFORMATION

### Corresponding Author

\*E-mail: [zhong.wang@mse.gatech.edu](mailto:zhong.wang@mse.gatech.edu).

## ■ ACKNOWLEDGMENT

Research was supported by DARPA (HR0011-09-C-0142, Program manager, Dr. Daniel Wattendorf), BES DOE (DE-FG02-07ER46394). Thanks to Ying Liu for discussion about the simulation. Z.L.W. and Q.Y. initiated the idea and designed the experiments. Q.Y. mainly carried out the experiments. W.H.W. and S.X. provided technical assistance. Z.L.W. and Q.Y. analyzed the data and wrote the paper.

## ■ REFERENCES

- (1) Fujii, T.; Gao, Y.; Sharma, R.; Hu, E. L.; DenBaars, S. P.; Nakamura, S. *Appl. Phys. Lett.* **2004**, *84*, 855.
- (2) Oder, T. N.; Kim, K. H.; Lin, J. Y.; Jiang, H. X. *Appl. Phys. Lett.* **2004**, *84*, 466.
- (3) Duan, X.; Huang, Y.; Agarwal, R.; Lieber, C. M. *Nature* **2003**, *421*, 241.
- (4) Duan, X.; Huang, Y.; Cui, Y.; Wang, J.; Lieber, C. M. *Nature* **2001**, *409*, 66.
- (5) Bao, J. M.; Zimmler, M. A.; Capasso, F.; Wang, X. W.; Ren, Z. F. *Nano Lett.* **2006**, *6*, 1719.
- (6) Park, W. I.; Yi, C. C. *Adv. Mater.* **2004**, *16*, 87.
- (7) Zimmler, M. A.; Stichtenoth, D.; Ronning, C.; Yi, W.; Narayanamurti, V.; Voss, T.; Capasso, F. *Nano Lett.* **2008**, *8*, 1695.
- (8) Xu, S.; Xu, C.; Liu, Y.; Hu, Y. F.; Yang, R. S.; Yang, Q.; Ryou, J. H.; Kim, H. J.; Lochner, Z.; Choi, S.; Dupuis, R.; Wang, Z. L. *Adv. Mater.* **2010**, *22*, 4749.
- (9) Wang, Z. L.; Yang, R.; Zhou, J.; Qin, Y.; Xu, C.; Hu, Y.; Xu, S. *Mater. Sci. Eng. R* **2010**, *70*, 320.
- (10) Wang, Z. L. *Nano Today* **2010**, *5*, 540.
- (11) Heo, Y. W.; Norton, D. P.; Tien, L. C.; Kwon, Y. S.; Kang, B. S.; Ren, F.; Pearton, S. J.; LaRoche, J. R.; et al. *Mater. Sci. Eng. R* **2004**, *47*, 1.
- (12) Zimmler, M. A.; Capasso, F.; Muller, S.; Ronning, C. *Semicond. Sci. Technol.* **2010**, *25*, 024001.
- (13) Soci, C.; Zhang, A.; Xiang, B.; Dayeh, S. A.; Aplin, D. P. R.; Park, J.; Bao, X. Y.; Lo, Y. H.; Wang, D. *Nano Lett.* **2007**, *7*, 1003.
- (14) Chen, M. W.; Chen, C. Y.; Lien, D. H.; Ding, Y.; He, J. H. *Opt. Express* **2010**, *18*, 14836.
- (15) Law, M.; Greene, L. E.; Johnson, J. C.; Saykally, R.; Yang, P. D. *Nat. Mater.* **2005**, *4*, 455.
- (16) Weintraub, B.; Wei, Y. G.; Wang, Z. L. *Angew. Chem., Int. Ed.* **2009**, *48*, 8981.
- (17) Wang, Z. L.; Song, J. H. *Science* **2006**, *312*, 242.
- (18) Cha, S. N.; Seo, J. S.; Kim, S. M.; Kim, H. J.; Park, Y. J.; Kim, S. W.; Kim, J. M. *Adv. Mater.* **2010**, *22*, 4726.
- (19) Wang, X. D.; Zhou, J.; Song, J. H.; Liu, J.; Xu, N. S.; Wang, Z. L. *Nano Lett.* **2006**, *6*, 2768.
- (20) Fei, P.; Yeh, P. H.; Zhou, J.; Xu, S.; Gao, Y. F.; Song, J. H.; Gu, Y. D.; Huang, Y. Y.; Wang, Z. L. *Nano Lett.* **2009**, *9*, 3435.
- (21) Zhou, J.; Fei, P.; Gu, Y. D.; Mai, W. J.; Gao, Y. F.; Yang, R.; Bao, G.; Wang, Z. L. *Nano Lett.* **2008**, *8*, 3973.
- (22) Yang, Y.; Qi, J. J.; Liao, Q. L.; Li, H. F.; Wang, Y. S.; Tang, L. D.; Zhang, Y. *Nanotechnology* **2009**, *20*, 125201.
- (23) Hu, Y. F.; Zhang, Y.; Chang, Y. L.; Snyder, R. L.; Wang, Z. L. *ACS Nano* **2010**, *4*, 4220.
- (24) Boxberg, F.; Sondergaard, N.; Xu, H. Q. *Nano Lett.* **2010**, *10*, 1108.
- (25) Yang, Q.; Guo, X.; Wang, W. H.; Zhang, Y.; Xu, S.; Lien, D. H.; Wang, Z. L. *ACS Nano* **2010**, *4*, 6285.
- (26) Gao, P.; Wang, Z. Z.; Liu, K. H.; Xu, Z.; Wang, W. L.; Bai, X. D.; Wang, E. G. *J. Mater. Chem.* **2009**, *19*, 1002.
- (27) Kim, K. K.; Lee, S. D.; Kim, H.; Park, J. C.; Lee, S. N.; Park, Y.; Park, S. J.; Kim, S. W. *Appl. Phys. Lett.* **2009**, *94*, 071118.
- (28) Pan, Z. W.; Dai, Z. R.; Wang, Z. L. *Science* **2001**, *291*, 1947.
- (29) Saleh, B. E. A.; Teich, M. C. *Fundamentals of Photonics*; Wiley-Interscience: New York, 1991.
- (30) Sze, S. M. *Physics of Semiconductor Devices*; Wiley-Interscience: New York, 1981.
- (31) Simon, J.; Protasenko, V.; Lian, C. X.; Xing, H. L.; Jena, D. *Science* **2010**, *327*, 60.
- (32) Liu, H. F.; Hu, G. X.; Gong, H.; Zang, K. Y.; Chua, S. J. *J. Vac. Sci. Technol., A* **2008**, *26*, 1462.
- (33) Hwang, D. K.; Kang, S. H.; Lim, J. H.; Yang, E. J.; Oh, J. Y.; Yang, J. H.; Parka, S. J. *Appl. Phys. Lett.* **2005**, *86*, 222101.
- (34) Nakayama, T.; Murayama, M. *J. Cryst. Growth* **2000**, *214/215*, 299.
- (35) Shi, L. B.; Cheng, S.; Li, R. B.; Kang, L.; Jin, J. W.; Li, M. B.; Xu, C. Y. *Mod. Phys. Lett. B* **2009**, *23*, 2339.
- (36) Shan, W.; Walukiewicz, W.; Ager, J. W.; Yu, K. M.; Zhang, Y.; Mao, S. S.; Kling, R.; Kirchner, C.; Waag, A. *Appl. Phys. Lett.* **2005**, *86*, 153117.
- (37) Zhang, Y.; Wen, Y. H.; Zheng, J. C.; Zhu, Z. Z. *Phys. Lett. A* **2010**, *374*, 2846.
- (38) Davydov, V. Y.; Averkiev, N. S.; Goncharuk, I. N.; Nelson, D. K.; Nikitina, I. P.; Polkovnikov, A. S.; Smirnov, A. N.; Jacobsen, M. A.; Semchinova, O. K. *J. Appl. Phys.* **1997**, *82*, 5097.
- (39) Suzuki, M.; Uenoyama, T. *J. Appl. Phys.* **1996**, *80*, 6868.
- (40) Guo, X.; Qiu, M.; Bao, J.; Wiley, B. J.; Yang, Q.; Zhang, X.; Ma, Y.; Yu, H.; Tong, L. *Nano Lett.* **2009**, *9*, 4515.
- (41) Born, M.; Wolf, E. *Principles of Optics*; Pergamon Press: Oxford, 1980.
- (42) Ebothe, J.; Gruhn, W.; Elhichou, A.; Kityk, I. V.; Dounia, R.; Addou, A. *Opt. Laser Technol.* **2004**, *36*, 173.
- (43) Vedam, K.; Davis, T. A. *Phys. Rev.* **1969**, *181*, 1196.
- (44) Zhu, G. A.; Yang, R. S.; Wang, S. H.; Wang, Z. L. *Nano Lett.* **2010**, *10*, 3151.
- (45) Nadarajah, A.; Word, R. C.; Meiss, J.; Konenkamp, R. *Nano Lett.* **2008**, *8*, 534.
- (46) Lim, J. H.; Kang, C. K.; Kim, K. K.; Park, I. K.; Hwang, D. K.; Park, S. J. *Adv. Mater.* **2006**, *18*, 2720.